

## **Corrosion Mitigation in Mature Reinforced Concrete Using Nanoscale Pozzolan Deposition**

**Henry Cardenas, Kunal Kupwade-Patil and Sven Eklund**

*Applied Electrokinetics Laboratory (AEL), Louisiana Tech University, Ruston, Louisiana  
71272, USA. E-mail: [cardenas@latech.edu](mailto:cardenas@latech.edu), [kvk001@latech.edu](mailto:kvk001@latech.edu), [seklund@latech.edu](mailto:seklund@latech.edu)*

### **ABSTRACT**

Electrokinetic Nanoparticle (EN) treatments were employed to mitigate corrosion in reinforced concrete. An electric field was used to drive pozzolanic nanoparticles through the capillary pores of concrete and directly to the reinforcement. The intent was to use the nanoparticles as pore blocking agents to prevent the ingress of chlorides. Effectiveness was examined for both freshly batched and relatively mature concrete. Cylindrical reinforced concrete specimens were subjected to EN treatment immediately after batching and then exposed to chlorides for a period of two years. The EN treated specimens exhibited a reduction in corrosion rates by a factor of 74 compared to the untreated controls. Other specimens were subjected to chlorides for a period of two years prior to EN treatment application. Electrochemical Chloride Extraction (ECE) and EN treatments were performed on these specimens for one week. These specimens were placed back into saltwater exposure for an additional year. The controls exhibited severe corrosion cracking compared to the treated specimens after one year of saltwater exposure. The corrosion rates were 8 times that of the treated specimens. This study demonstrated that microstructural changes due to treatment were effective in mitigating reinforcement corrosion in both young and mature concrete.

### **INTRODUCTION**

This work deals with the application of pozzolanic nanoparticles to mitigate reinforcement corrosion in concrete. Durability of reinforced concrete is one of the major concerns in the civil infrastructure industry [Broomfield 1997]. The porous nature of concrete leads to the ingress of harmful species like chlorides and sulfates, which can lead to the deterioration of the structure. A new sustainable solution is to fill these pores with nanoparticles to reduce porosity and increase strength [Cardenas and Kupwade-Patil 2007, Kupwade-Patil and Cardenas 2008, Kupwade-Patil *et al.*, 2008]. This work involved the application of an electric field to drive the nanoparticles to the reinforcement. This process is known as electrokinetic nanoparticle (EN) treatment. It is illustrated in Figure 1. This concept uses electrophoresis and ionic conduction to carry pore-blocking agents into the capillary pores of concrete.

Earlier work examined the impact on reinforcement corrosion when 24-nm pozzolanic nanoparticles were driven into the capillary pores of relatively immature concrete as shown in Figure 1 [Kupwade-Patil 2007]. Steel reinforced cylindrical concrete specimens were subjected to initial saltwater exposure followed by electrochemical chloride extraction and

EN treatment. The nanoparticles acted as pore blocking agents while reducing the porosity and increasing the strength of the concrete.

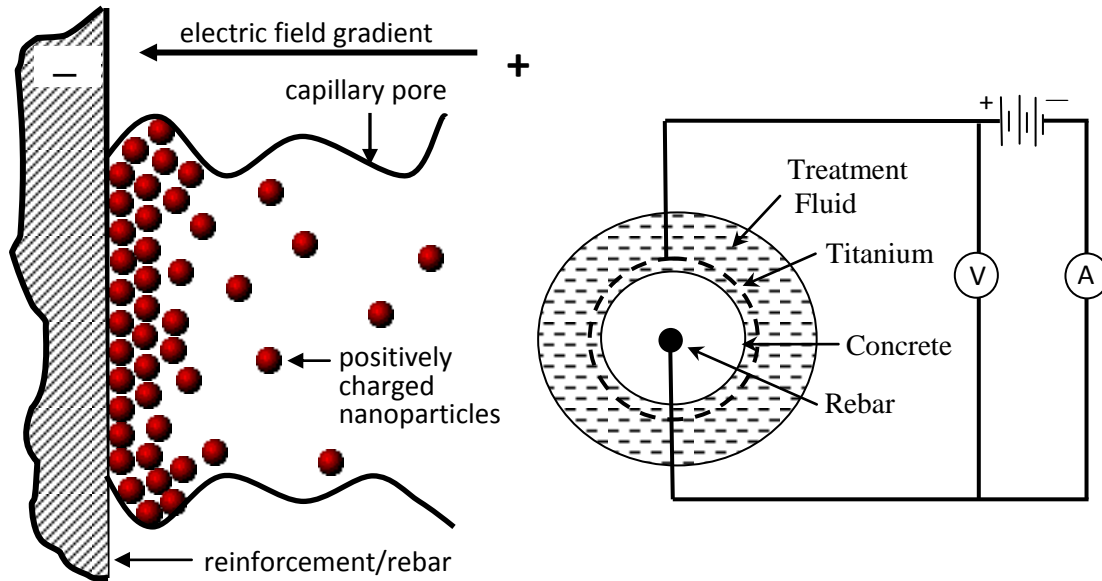


**Fig 1. Concept of Nanoparticle Transport into Capillary Pores and the EN Treatment Circuit**

## EXPERIMENTAL PROCEDURE

Both young and mature cylindrical reinforced concrete specimens were cast 6 inch [0.15 m] high by 3 inch [0.07 m] in dia. using type I Portland cement. Young specimens (freshly batched concrete) were subjected to 7 days of EN treatment using a current density of  $1 \text{ A/m}^2$ . These specimens were then subjected to 36 months of wet and dry saltwater exposure as shown in Table 1. The wet and dry cycle consisted of 14 days of 3.5 % NaCl solution exposure (wet cycle) followed by lab air exposure for 14 days (dry cycle). Mature specimens were first subjected to 1 year of initial wet-dry saltwater exposure. After this period, chlorides were extracted from six specimens for 7 days followed by 7 days of EN treatment using alumina coated silica nanoparticles with a current density of  $1 \text{ A/m}^2$ . The circuit used for EN treatment is shown in Figure 1. The positive pole of the power supply was connected to the titanium ring surrounding the reinforcement and the negative pole was connected directly to the 1018 steel rebar. After EN treatment the specimens were subjected to 735 days of 14 day, wet-dry, saltwater exposure cycles as shown in Table 1.

The corrosion potential of the steel was measured by with respect to a ( $\text{Cu/CuSO}_4$ ) reference electrode. Linear polarization resistance (LPR) analysis was used to measure the corrosion current density ( $I_{\text{corr}}$ ) with a Solartron potentiostat (model no. 1287) manufactured by Roxboro Company, UK. Chloride diffusion coefficients were measured using electrochemical impedance spectroscopy [Marcus and Mansfeld 2005, Shi *et al.* 1999]. Indirect tension testing was conducted as per ASTM C 496-96. These tests were used to compare the tensile strength of the EN treated specimens as compared to the controls. This test method consisted of the application of a diametrical compressive force distributed along the length of the cylinder at a rate of 150 psi/min until failure.

**Table1. Schedule of Treatments for Young and Mature concrete**

Specimen Type	Time (Years)		
	1	2	3
Mature Concrete	Saltwater Exposure	EN	Saltwater Exposure
Young Concrete	EN	Saltwater Exposure	
Controls (Young and Mature Concrete)	Saltwater Exposure		

ASTM G33-99 was followed to conduct the visual examination of the steel reinforcement immediately after the indirect tension test. ASTM C1152 was followed to measure the acid soluble chloride content at various distances from the reinforcement. Porosity measurements were conducted on samples taken from tensile test specimens. Powdered samples of 5-7g were ground to pass a No.30 sieve. These particles were collected and dried to obtain a porosity measurement via weight loss at 105°C. Finely ground concrete samples were mixed with DI water and titrated against 0.1 N HCl. Phenolphthalein were used as an indicator for a color change between pH values of 8 to 9.6 and alizarin yellow from 10.1 to 12. Microscopic imaging samples were extracted from the broken concrete cylinders and mounted in epoxy. Polishing was conducted using 60, 120, 150, 320 and 600 grit size papers with Alpha-beta Polisher manufactured by Buehler, Lake Bluff, IL. Micro-polishing was conducted with Buehler polishing-cloths in the range of 15-1µm using a non-aqueous lubricant (propylene glycol). After each stage of polishing the specimens were rinsed in ethyl alcohol to remove loose material. Microstructural analysis was conducted using a Hitachi S-4800 field emission scanning electron microscope (FE SEM). Quantitative elemental analysis was done using Genesis Microanalysis software manufactured by Ametek Inc. Fourier transform infrared spectroscopy (FTIR) was conducted on finely ground samples using a Nicolet IR-100 FTIR spectrometer from Thermo Scientific Inc., Waltham, MI. X-Ray diffraction on powdered samples was conducted using a Bruker AXS Inc, Billerica, MI.

**RESULTS AND DISCUSSION**

The corrosion potentials and corrosion rates of the reinforced concrete specimens are shown in Figure 2. Average corrosion potentials of -1544 mV and -1284 mV were observed for mature and young control specimens at the end of 1100 days of saltwater exposure. After saltwater exposure the mature EN treated specimens demonstrated an average corrosion potential of -845 mV and young specimens yielded -819 mV. The lower corrosion potentials exhibited by the EN treated specimens indicated a likelihood of less active corrosion as compared to the untreated controls.

The corrosion current densities ( $I_{corr}$ ) were measured following 250, 500, 750 and 1100 days of saltwater exposure using the linear polarization resistance (LPR) technique. Average  $I_{corr}$  values of 57 and 1.3 were observed in the young and mature controls respectively after 250 days of exposure, while the young and mature EN Treated specimens showed 0.2 and 0.7 respectively. Comparison of these values with the reference values of Table 2 shows that the reinforcement of the controls was highly corroded as compared the EN treated specimens which exhibited low to moderate corrosion. High  $I_{corr}$  values of 1264 and 89 for the mature and young controls were significantly higher than the respective EN treated specimens (160 and 1.28 ) at the end of 1100 days of

exposure. These values indicate that the mature and young EN treated specimens exhibited a lower corrosion rates by factor of 8 and 74 as compared to their respective untreated controls.

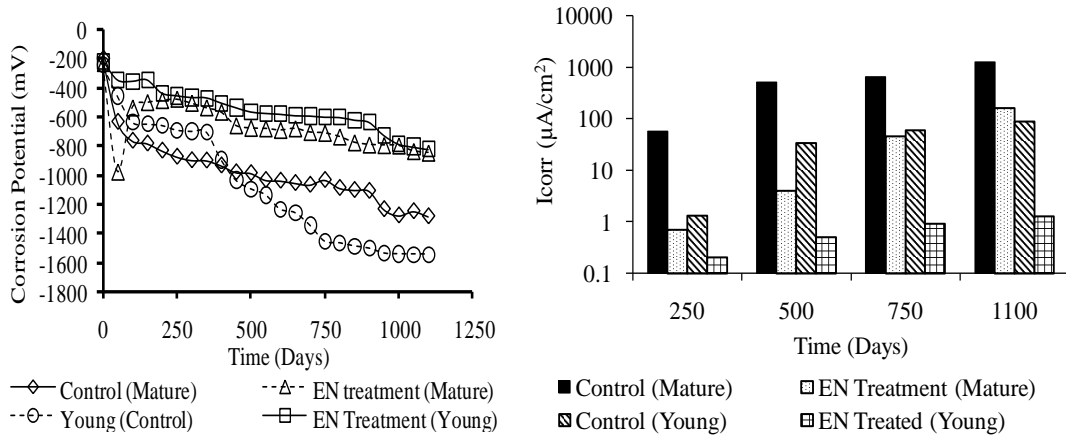


**Fig 2. Corrosion Potentials and Corrosion Current Densities ( $I_{corr}$ ) of EN Treated and Control Specimens of Mature and Young Concrete**

The chloride diffusion coefficients for the reinforced concrete specimens are shown in Figure 3A. Diffusion coefficients of  $2.34 \times 10^{-14} \text{ m}^2/\text{s}$  (Young EN Treated),  $6.50 \times 10^{-13} \text{ m}^2/\text{s}$  (Mature EN Treated),  $2.30 \times 10^{-13} \text{ m}^2/\text{s}$  (Young Control) and  $8.69 \times 10^{-12} \text{ m}^2/\text{s}$  (Mature Control) were observed. Bentur and others obtained a chloride diffusion coefficient for unprotected concrete (0.5 w/c ratio) of [Bentur *et al.*, 1997]. This diffusion coefficient was calculated to result in corrosion initiation in 17 years. This value used in the current study as a bench mark for assessing chloride diffusion coefficients. The mature control specimens exhibited higher chloride diffusion coefficients as compared to this benchmark level where as the young control specimens ( did not exceed this benchmark until after 500 days of saltwater exposure. In contrast, the EN treated specimens exhibited significantly lower diffusion coefficients as compared to the benchmark, indicating that the nanoparticles would be expected to inhibit the re-entry of chlorides.

The mature control specimens and EN treated specimens are shown in Figure 3B after 1100 days of saltwater exposure. The controls exhibited corrosion induced cracking where as the EN treated specimens exhibited no signs of cracking. Images of the steel bars removed from the mature specimens after the splitting tensile test are shown in Figure 4. The EN treated specimens exhibited corrosion products covering an average of 14 % of their surfaces while the control specimens showed an average corrosion product coverage of 99 %. Young EN treated concrete exhibited a 0.3 % corrosion product coverage (See Figure 5). In comparison the young untreated controls had a corrosion product coverage that averaged 96 %. Based on these observations the EN treatment was found to inhibit the return of chlorides and significantly slowed the reinforcement corrosion rate in concrete. Results for splitting tensile strength, porosity, pH and corrosion rates are shown in Table 3. The mature EN treated specimens exhibited a 50 % increase in strength while the young EN treated specimens showed a 14 % increase in strength as compared to their respective controls.

The mature and young EN treated specimens exhibited 8 % and 5 % porosities while the controls exhibited respective values of 11 and 9 %. The mature and young EN treated specimens yielded porosity reductions of 27 % and 44 % as compared to the untreated controls. pH values of 11.3 (mature) and 11.8 (young) were observed among the EN treated

specimens. The controls showed values of 8.1 (mature) and 8.4 (young). The threshold pH value for corrosion initiation is 11.0 [Broomfield 1997]. This indicates that EN treatment was effective in keeping the pH value above the significant corrosion initiation limit and hence slowing the carbonation process. The corrosion rates at the end of 1100 days of post treatment saltwater exposure are also shown in Table 3.

**Table 2. Interpretation of Corrosion Current with Corrosion (Adapted from Broomfield 1997)**

Corrosion Current Density ( $\mu\text{A}/\text{cm}^2$ )	Corrosion
< 0.1	Negligible
0.1-0.5	Low
0.5-1.0	Moderate
> 0.1	High

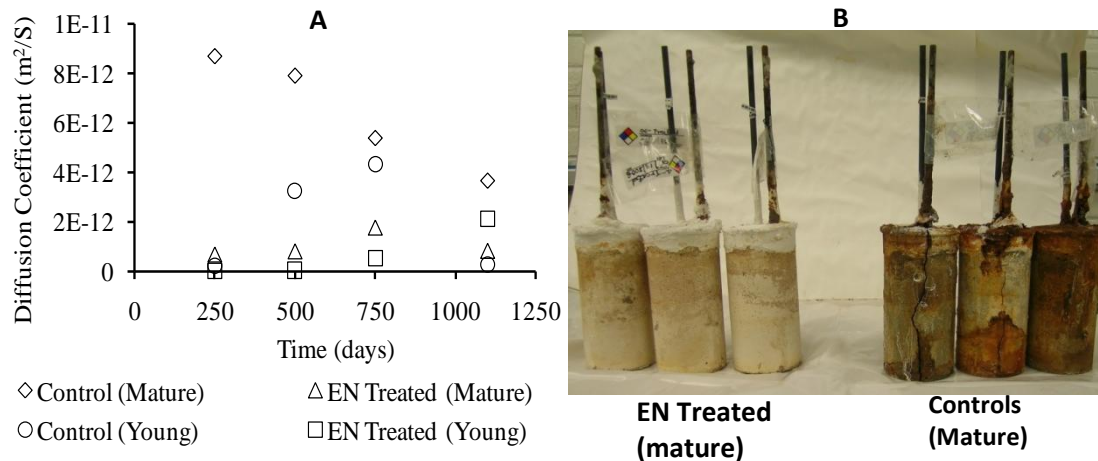
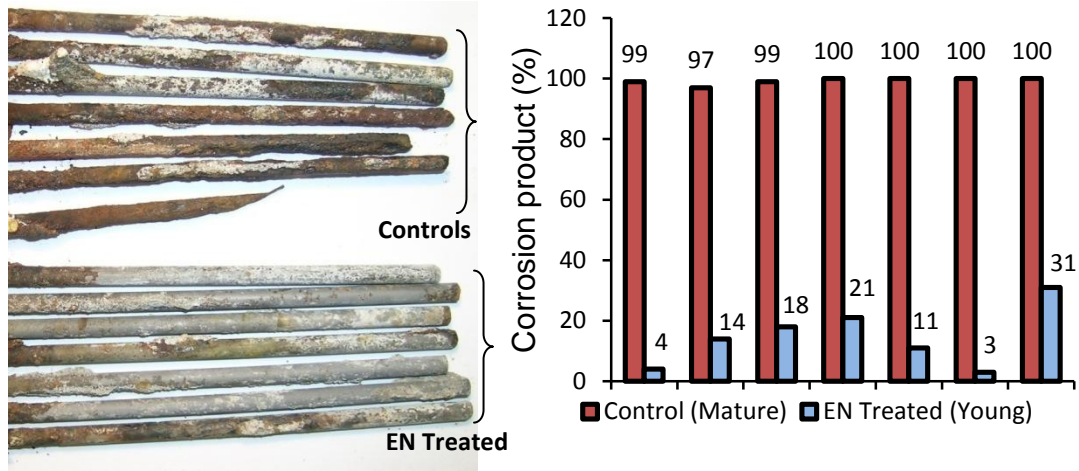


**Fig 3. A. Chloride Diffusion Coefficient obtained using Electrochemical Impedance Spectroscopy (EIS) for both Mature and Young Concrete; B. Front View of the Mature Un-cracked EN Treated Cylindrical Specimens and Cracked Controls**

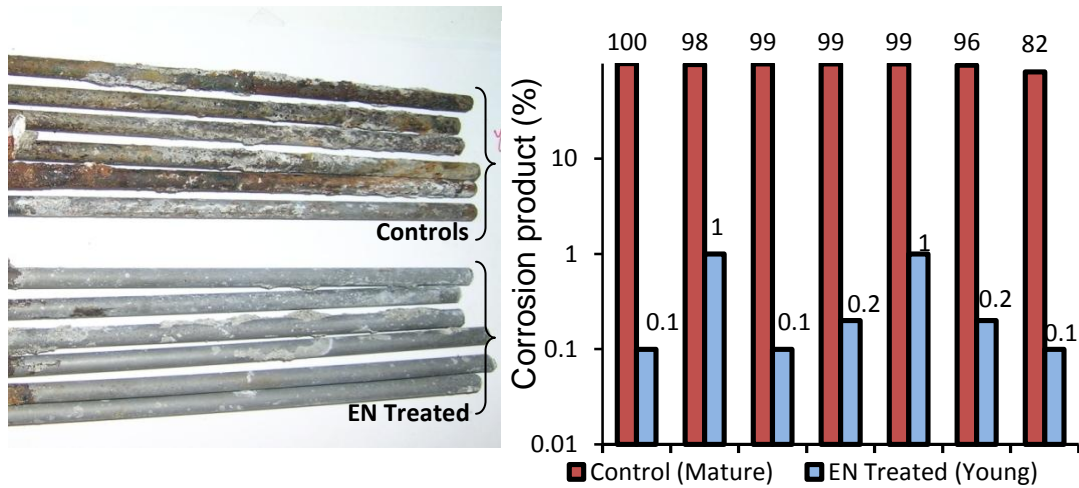
The mature control and EN treated specimens exhibited high corrosion rates at the end of post treatment saltwater exposure period. These specimens were exposed to one year of wet-dry salt water exposure before receiving EN treatment. It is conceivable that the relatively short duration of the treatment was probably insufficient to remove enough chlorides needed for protection since most chloride extraction operations run 6-8 weeks. In contrast, the young EN treated specimens exhibited lower corrosion rates by a factor of 74 at the end of post saltwater exposure. These specimens had much less opportunity to absorb large quantities of chloride. Based on these observations it appears that the porosity and corrosion results indicated that the EN treatment was effective in sustaining an elevated pH while reducing the corrosion rates presumably through a reduction in porosity.

The chloride contents at various distances from the rebar are shown in Figure 6. The young and mature control specimens exhibited chloride contents of 0.16 and 0.21 % by mass of cement. The allowable threshold chloride content as per ASTM C 1152 is 0.10 %. In contrast, the chloride contents of 0.01% (mature EN treated) and 0.03 % (young EN treated)

were well below the allowable threshold level of 0.10 % by mass of cement. In considering the chloride diffusion coefficients from Figure 3A together with these chloride contents it is clear that the EN treatment was effective in retarding the ingress of the chlorides during the post treatment saltwater exposure period.



**Fig 4. Corrosion Product Coverage Areas Measured on Steel Bars taken from Control Specimens and EN Treated Specimens of Mature Concrete**

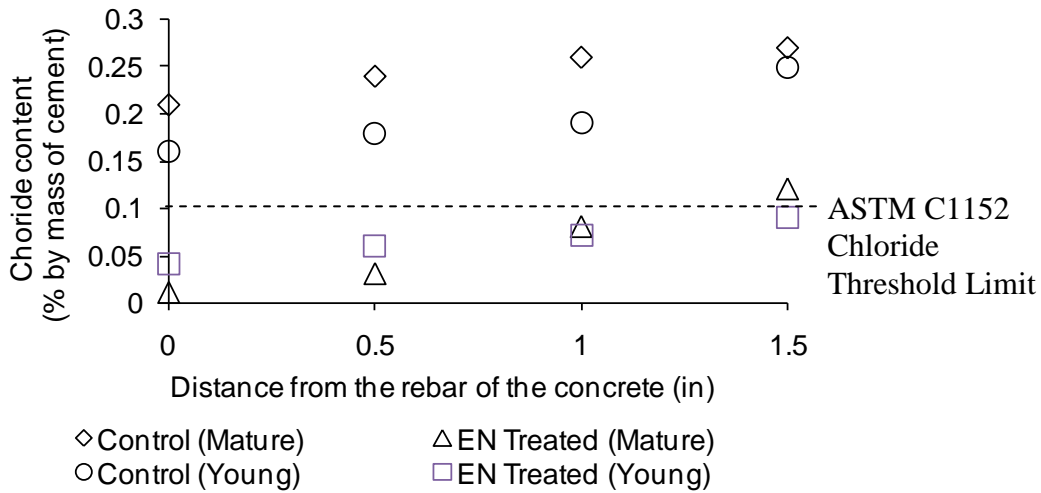


**Fig 5. Corrosion Product Coverage Areas Measured on Steel Bars taken from Control Specimens and EN Treated Specimens of Young Concrete**

**Table 3. Strength, Porosity and Corrosion Analysis**

Treatment Type	Strength (psi)	Porosity (%)	pH	Corrosion Covered Area (%)	Corrosion Rate (mpy)
Control (Mature)	263	11	8.1	99	517
EN Treated (Mature)	535	8	11.3	15	66
Control (Young)	583	9	8.4	96	37
EN Treated (Young)	680	5	11.8	0.3	0.5

In Figure 7A scanning electron microscopy (SEM) conducted on the control specimens indicated the presence of ettringite needles in the vicinity of hexagonal shaped calcium hydroxide (Taylor 1997). The further magnified image of ettringite is shown in Figure 7B. Figures 8A and B show an EN treated specimen with a dense morphology at the rebar concrete interface as compared to the more porous control specimens. The dense morphology indicates that the EN treatment was effective in reduction of porosity and increasing strength.

**Fig 6. Variation of Chloride Contents with Distance from the Reinforcement**

In Figure 9 the polished young EN treated specimen exhibited the presence of calcium silicate hydrate (C-S-H) inter-percolated with calcium carbonate (manifesting as a white powdery phase). The Energy Dispersive Spectroscopy (EDS) analysis indicates peaks of alumina, silica, calcium, chlorine, oxygen and carbon. This evidence together with the earlier noted pH value of 8.1 (which is below the threshold limit of 11 for corrosion initiation) further supports the suspected carbonation process.

SEM micrograph of a polished untreated young control shows the presence of chloride peaks but no aluminum peaks as shown in Figure 10. Backscattered electron image (BSE) imaging confirms the presence of dicalcium aluminate hydrate ( $C_2AH_8$ ) inside the pore in Figure 11. The curving striated needles of dicalcium aluminate hydrate is shown at higher magnification in Figure 12. While the nanoparticles appear to act as pore blocking agents they also appear to be forming strength increasing phases such as  $C_2AH_8$ .



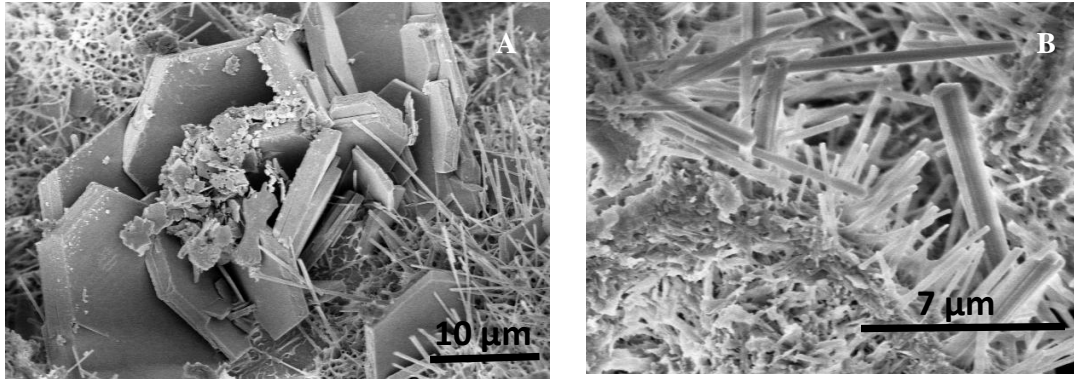


**Fig 7. Ettringite in the Presence of Calcium Hydroxide of Mature Concrete.  
B. Ettringite Needles in the Mature Concrete Specimens**

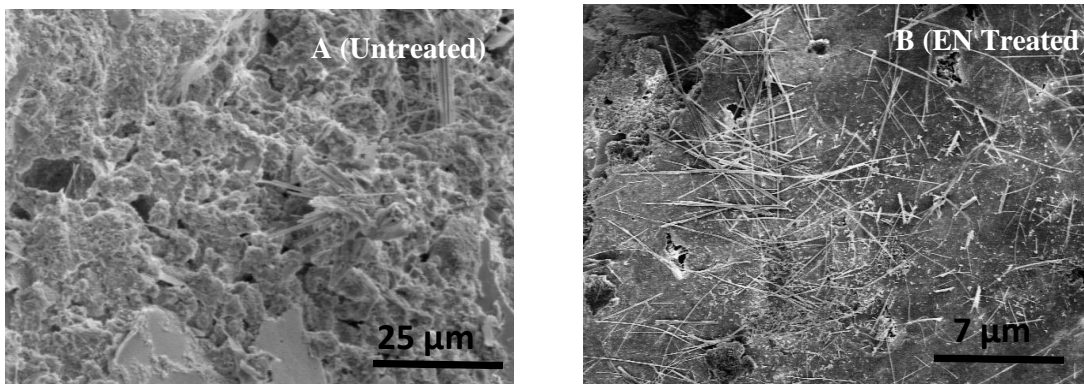


**Fig 8. Morphology of an Untreated specimen compared to an EN Treated specimen that exhibited a more dense morphology.**

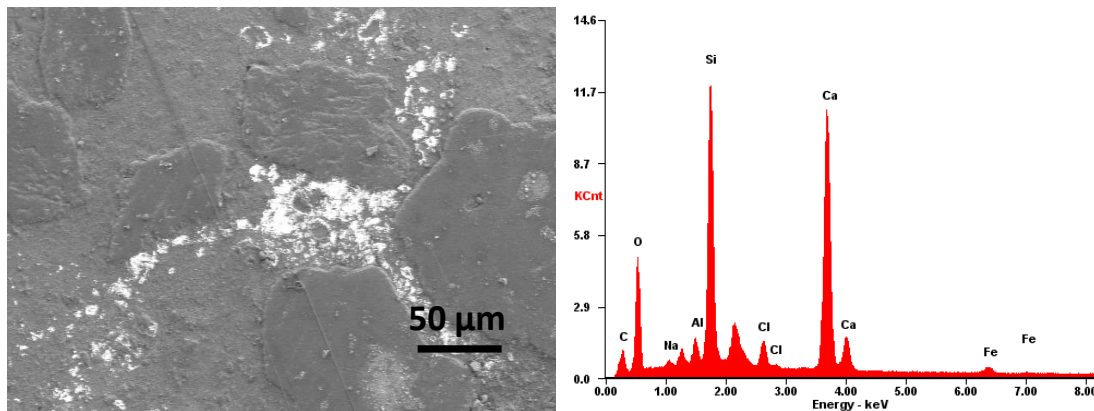


**Fig 9. Backscattered Electron Image (BSE) of a Young EN Treated specimen. Brighter Regions indicate C-S-H mixed with Calcium Carbonate ( $\text{CaCO}_3$ )**

Fourier transform infra-red (FTIR) spectra are shown in Figure 13. The mature and young EN Treated specimens exhibited strong broad peaks ranging from  $3400$  to  $3600\text{ cm}^{-1}$  which indicate calcium aluminate hydrate (C-A-H), while the untreated controls did not show any such peaks in this region [Fernandez-Carrasco et al. 2008, Yu et al. 1999]. Based on these



observation it appears that the alumina coated silica nanoparticles reacted with the calcium hydroxide, forming C-A-H which is a metastable strength enhancing phase.

X-Ray diffraction results indicated the presence of gehlenite hydrate ( $C_2ASH_8$ ), C-S-H on the young EN treated specimens while both young and mature EN Treated specimens showed the presence of xonotlite as shown in Figure 14. Gehlenite hydrate is formed by the reaction of silicate ions with the calcium aluminate hydrate phases [Taylor 1997]. Unidentified phases may also be formed by the combination of C-S-H and aluminium rich gel. Further study is required to elucidate these phases. Xonotlite forms as a hydration product of semi-crystalline C-S-H [Nocun-Wczelik 1999]. Additionally tobermorite can be gradually transformed into xonotlite at elevated temperatures. The EN treated specimens also exhibited ettringite ( $6.CaO.Al_2O_3.3SO_3.32H_2O$ ). The untreated controls also exhibited the presence of C-S-H, calcium hydroxide and ettringite. Based on these observations the EN treatment using alumina coated silica nanoparticles was successful in reducing reinforcement corrosion in concrete by blocking pores and by producing porosity reducing phases such as calcium aluminate hydrate (C-A-H) and C-S-H.

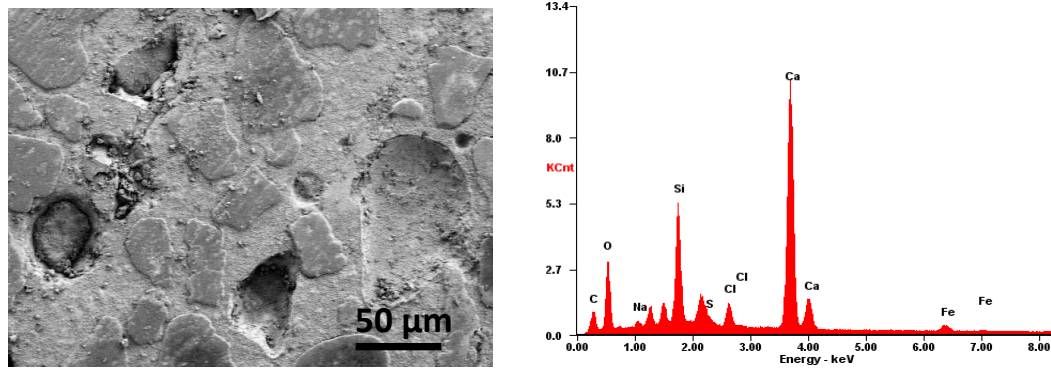


**Fig 10. Backscattered Electron Image (BSE) of the Young Control specimen depicting degradation and EDS Spectrum**

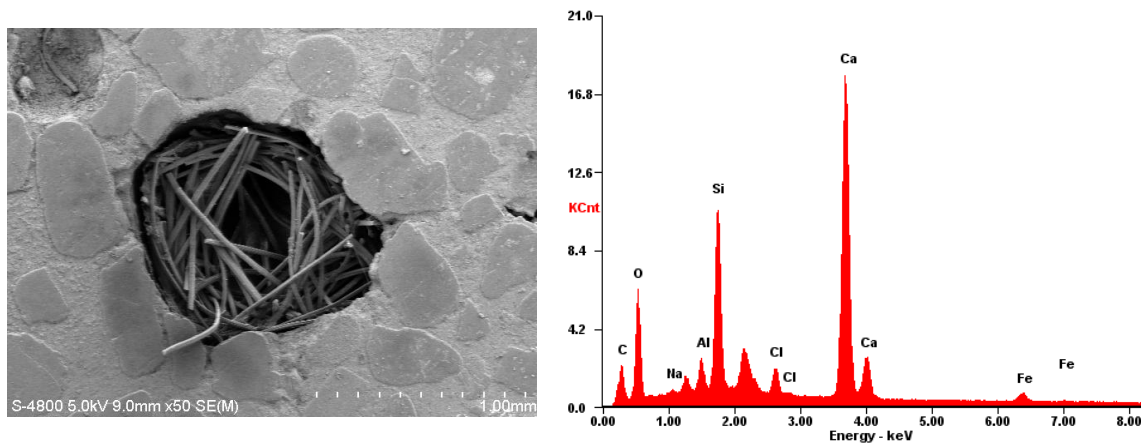


**Fig 11. Presence of Dicalcium Aluminate Hydrate ( $C_2AH_8$ ) on the Young EN Treated Specimen**



**Fig 12. Magnified Image showing Striated Needles of Dicalcium Aluminate Hydrate (C<sub>2</sub>AH<sub>8</sub>)**

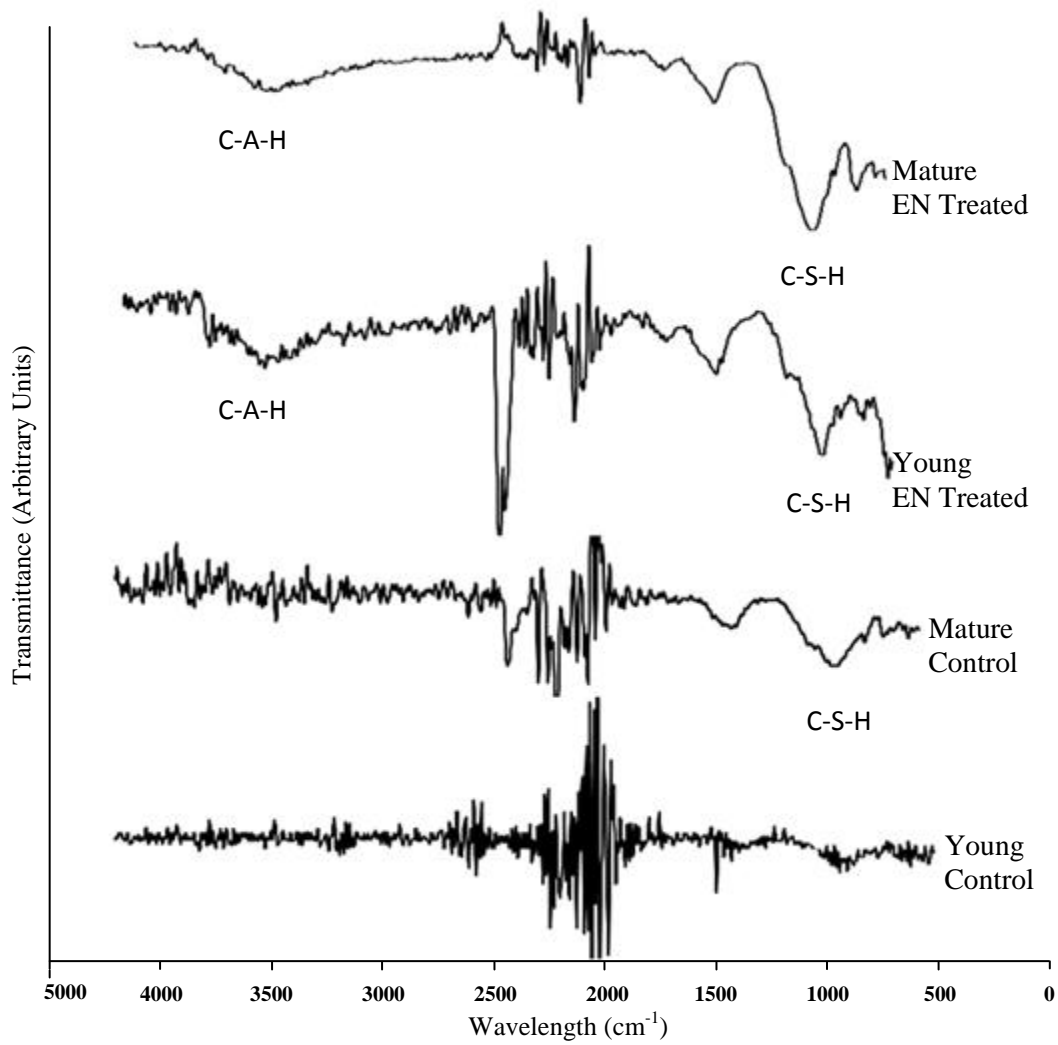


**Fig 13. Fourier Transform Infrared Spectroscopy (FTIR) of the EN Treated and Control Specimens**

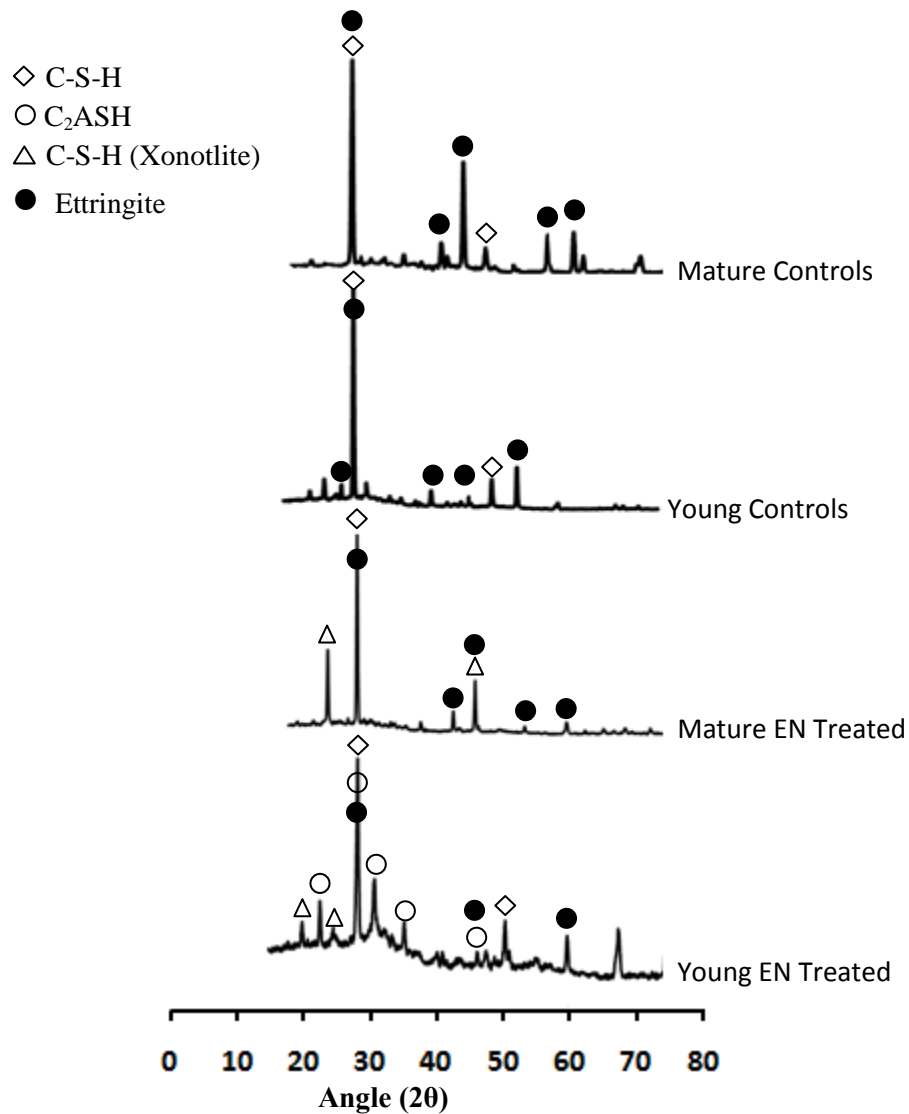


**Fig 14. XRD Data of EN Treated and Control Specimens**

## CONCLUSION

Strength, porosity, and corrosion rate results indicate that the EN treatment was effective in keeping the pH and chloride content below threshold levels. SEM, FTIR and XRD examinations indicate that C-S-H and C-A-H were formed during treatment which played a role in raising the tensile strength. EN treatment was found useful in mitigating reinforcement corrosion in both relatively mature and young concrete.

## REFERENCES

ASTM C 496/96. "Standard Test Method for Splitting Tensile Strength of Cylindrical Concrete Specimens." *ASTM International, West Conshohocken, PA*, 5 pages.

- ASTM G33/99. "Standard Practice for Recording Data from Atmospheric Corrosion Test of Metallic-Coated Steel Specimens." *ASTM International, West Conshohocken, PA*, 3 pages.
- ASTM C 1152. "Standard Test Method for Acid- soluble Chloride in Mortar and Concrete", *ASTM International, West Conshohocken, PA*, 4 pages.
- Bentur, A., Diamond, S., and Berkle, N. (1997). "Steel Corrosion in Concrete." 1<sup>st</sup> Ed, E & FN Spon.
- Broomfield, J. (1997). "Corrosion of Steel in Concrete, Understanding, Investigation and Repair." 1st Ed, E & FN Spon.
- Cardenas, H., and Kupwade-Patil, K. (2007). "Corrosion Remediation using Chloride Extraction Concurrent with Electrokinetic Pozzolan Deposition in Concrete." *Proceedings of the Sixth International Conference on Electrokinetic Remediation*, 117.
- Cardenas, H., and Struble, L.(2006). "Electrokinetic Nanoparticle Treatment of Hardened Cement Paste for Reduction of Permeability," *Journal of Materials in Civil Engineering*, 18(1), July-August, 554-560.
- Fernandez-Carrasco, L., Rius, J., and Miravittles. (2008). "Supercritical Carbonation of Calcium Aluminate Cement." *Cement and Concrete Research*, 38(8-9), 1033-1037.
- Kupwade-Patil, K. (2007). "A New Corrosion Mitigation Strategy using Nanoscale Pozzolan Deposition." Masters Thesis, Louisiana Tech University.
- Kupwade-Patil, K and Cardenas, H. (2008). "Corrosion Mitigation in Concrete Using Electrokinetic Injection of Reactive Composite Nanoparticles." *Proceeding of 53 International Conference on Advancement of Material and Process Engineering*, 11 pages.
- Kupwade-Patil, K., Gordan, K., Xu, K., Moral, O., Cardenas, H., and Lee, L. (2008) "Corrosion mitigation in concrete beams using electrokinetic nanoparticle ." *Proceedings of First International Conference on Excellence in Concrete Construction Through Innovation*, 365-371.
- Marcus, P., and Mansfield, F. (2005). "Analytical Methods in Corrosion Science and Engineering." 1st Ed., CRC Press.
- Nocun-Wczelik.(1999). "Effect of Na and Al on the Phase Composition and Morphology of Autoclaved Calcium Silicate Hydrates," *Cement and Concrete Research*, 29(11), 1759-1767.
- Shi, M., Chen, Z., and Sun, J., (1999) "Determination of chloride diffusivity in concrete by AC Impedance spectroscopy." *Cement and Concrete Research*, 29(7), 1111-1115.
- Taylor, H.F.W (1997). *Cement Chemistry*, 2nd Ed., Thomas Telford.
- Yu, P., Kirkpatrick, J., Poe, B., McMillan, P., and Cong, X. (1999), "Structure of Calcium Silicate Hydrate (C-S-H) Near, Mid and Far-Infrared Spectroscopy," *Journal of American Ceramic Society*, 82(3), March, 742-748.